The Plant Cell, Vol. 18, 2035–2050, August 2006, www.plantcell.org © 2006 American Society of Plant Biologists

Functional Replacement of Ferredoxin by a Cyanobacterial Flavodoxin in Tobacco Confers Broad-Range Stress Tolerance [W]

Vanesa B. Tognetti,[a] Javier F. Palatnik,[a] María F. Fillat,[b] Michael Melzer,[c] Mohammad-Reza Hajirezaei,[c] Estela M. Valle,[a] and Néstor Carrillo[a,1]

[a] Instituto de Biología Molecular y Celular de Rosario, Consejo Nacional de Investigaciones Científicas y Técnicas, División Biología Molecular, Facultad de Ciencias Bioquímicas y Farmacéuticas, Universidad Nacional de Rosario, S2002LRK Rosario, Argentina

[b] Departamento de Bioquímica y Biología Molecular y Celular, Facultad de Ciencias, Universidad de Zaragoza, 50009 Zaragoza, Spain

[c] Institut für Pflanzengenetik und Kulturpflanzenforschung, 06466 Gatersleben, Germany

Chloroplast ferredoxin (Fd) plays a pivotal role in plant cell metabolism by delivering reducing equivalents to various essential oxidoreductive pathways. Fd levels decrease under adverse environmental conditions in many microorganisms, including cyanobacteria, which share a common ancestor with chloroplasts. Conversely, stress situations induce the synthesis of flavodoxin (Fld), an electron carrier flavoprotein not found in plants, which can efficiently replace Fd in most electron transfer processes. We report here that chloroplast Fd also declined in plants exposed to oxidants or stress conditions. A purified cyanobacterial Fld was able to mediate plant Fd-dependent reactions in vitro, including $NADP^+$ and thioredoxin reduction. Tobacco (*Nicotiana tabacum*) plants expressing Fld in chloroplasts displayed increased tolerance to multiple sources of stress, including redox-cycling herbicides, extreme temperatures, high irradiation, water deficit, and UV radiation. Oxidant buildup and oxidative inactivation of thioredoxin-dependent plastidic enzymes were decreased in stressed plants expressing plastid-targeted Fld, suggesting that development of the tolerant phenotype relied on productive interaction of this flavoprotein with Fd-dependent oxidoreductive pathways of the host, most remarkably, thioredoxin reduction. The use of Fld provides new tools to investigate the requirements of photosynthesis in planta and to increase plant stress tolerance based on the introduction of a cyanobacterial product that is free from endogenous regulation in higher plants.

INTRODUCTION

Ferredoxins (Fds) are ubiquitous iron–sulfur proteins involved in many different electron transfer pathways in plants, animals, and microorganisms (Knaff, 2005). As the major low-potential mobile electron carrier protein of chloroplasts, Fd plays a central role in the physiology of the plant cell, distributing the reducing equivalents generated in the photosynthetic electron transport chain (PETC) to various electron-consuming reactions of the chloroplast. Part of the Fd reduced at the level of photosystem I (PSI) delivers reducing equivalents to ferredoxin-$NADP^+$ reductase (FNR) for $NADP^+$ photoreduction, generating the NADPH needed for CO_2 fixation and other biosynthetic routes, but a substantial fraction engages in electron transfer to alternative plastidic enzymes involved in crucial cellular pathways. They include nitrogen and sulfur assimilation via Fd-dependent nitrite reductase and sulfite reductase as well as amino acid and fatty acid metabolism through Gln-oxoglutarate amino transferase and fatty acid desaturase. Reductive activation of key chloroplast enzymes by the thioredoxin (Trx)/ferredoxin-thioredoxin reductase (FTR) system also requires a steady supply of Fd to ensure proper function of the Calvin cycle, the malate valve, and several other metabolic and dissipative processes (Balmer et al., 2003). In addition, Fd is a key player in different routes of cyclic electron flow that operate under physiological and stress conditions to eliminate the excess of reducing power and prevent uncontrolled overreduced states in the PETC and the stroma (Kramer et al., 2004; Munekage et al., 2004). The Fd redox state also functions as a signal in the intracellular signaling pathway between chloroplast and nucleus (Knaff, 2005). The various Fd acceptors are organized in a hierarchical manner, attaining their maximal activities at different electronic pressures (Backhausen et al., 2000). Most of these Fd activities are also found in eukaryotic algae and in cyanobacteria, the closest living relatives of the ancient endosymbiont that gave origin to chloroplasts (Falk et al., 1995).

In agreement with this multiplicity of functions, Fd accumulates above the tight stoichiometry of its redox partners in the

[1] To whom correspondence should be addressed. E-mail carrillo@ibr.gov.ar; fax 54-341-4390465.

The author responsible for distribution of materials integral to the findings presented in this article in accordance with the policy described in the Instructions for Authors (www.plantcell.org) is: Néstor Carrillo (carrillo@ibr.gov.ar).

[W] Online version contains Web-only data.

Article, publication date, and citation information can be found at www.plantcell.org/cgi/doi/10.1105/tpc.106.042424.

PETC (PSI, FNR) in both plants (Bohme, 1978) and algae (Inda and Peleato, 2002). The amounts of Fd in photosynthetic microorganisms fluctuate in response to different environmental stimuli, including light-dependent induction (Mazouni et al., 2003), and downregulation by iron starvation, environmental adversities, and oxidative stress episodes (Erdner et al., 1999; Mazouni et al., 2003; Singh et al., 2004). In higher plants, Fd is encoded by a small gene family whose members display tissue-specific expression and perform specialized tasks in different organs (Hanke et al., 2004). Chloroplast Fd is also induced by light, through a redox-based mechanism (Petracek et al., 1998). Repression of Fd expression by hostile environmental situations has not yet been reported for plants. However, genome-wide analysis of *Arabidopsis thaliana* transcription profiles indicates that steady state levels of transcripts encoding Fd are decreased, relative to control conditions, under virtually all kinds of abiotic stress (Zimmermann et al., 2004). Such an effect could deeply affect central metabolic pathways of the chloroplast and the cell and contribute to the growth penalties exhibited by plants exposed to adverse conditions. Transgenic potato (*Solanum tuberosum*) plants in which the contents of Fd were diminished by the expression of antisense RNA displayed lower CO_2 assimilation rates, growth arrest, and altered distribution of reducing equivalents to oxidoreductive pathways of the stroma (Holtgrefe et al., 2003).

Although each of the various stress conditions to which a plant may be subjected has distinctive characteristics and elicits its own specific responses, they share a common feature: the establishment of an oxidative situation that accounts for a substantial part of the damage inflicted upon the stressed organism. NADPH-consuming reactions of photosynthesis are early targets of inhibition by most environmental hardships. As a consequence, $NADP^+$ levels decline, leading to overreduction of the PETC as its terminal acceptor becomes unavailable (Allen, 1995; Apel and Hirt, 2004). Reduced intermediates of the chain may then engage in energy and electron transfer to adventitious acceptors, most conspicuously oxygen, resulting in the generation of reactive oxygen species (ROS), such as superoxide radicals, H_2O_2, hydroxyl radicals, and carbon-based organic radicals (Allen, 1995).

Photosynthetic microorganisms have adapted to the undesirable consequences of Fd decline under stress by inducing the expression of isofunctional electron carriers termed flavodoxins (Flds), small soluble proteins (~19 kD) containing one molecule of noncovalently bound flavin mononucleotide as a prosthetic group (Falk et al., 1995). Cyanobacterial Fld has been shown to efficiently replace Fd in $NADP^+$ photoreduction, nitrogen fixation, sulfite reduction, and the phosphoroclastic reaction (Falk et al., 1995). Unlike FNR and Fd, which are widely distributed among plastids, mitochondria, and bacteria, Flds are restricted to prokaryotes and some eukaryotic algae (Erdner et al., 1999). In cyanobacteria and enterobacteria, Fld levels increase severalfold on exposure of the cells to the redox-cycling herbicide methyl viologen (MV) and other superoxide-propagating compounds (Zheng et al., 1999; Yousef et al., 2003; Singh et al., 2004), and overexpression of the flavoprotein in *Escherichia coli* leads to augmented tolerance toward various sources of oxidative stress (Zheng et al., 1999).

Somewhere in the evolutionary path that led to the appearance of vascular plants, the Fld gene disappeared from the plant genome (Arabidopsis Genome Initiative, 2000) and the considerable advantages derived from its expression and function were lost or became dispensable. Interestingly, at least some of the plant enzymes whose bacterial ancestors used Fld as a normal or occasional substrate have retained the ability to efficiently interact with this electron carrier in vitro, with chloroplast FNR being a conspicuous example (Nogués et al., 2004). The aim of this research, therefore, was twofold: to investigate the effects of adverse environments on the contents of chloroplast Fd, and to determine whether bacterial Fld could also exert its protective functions in planta. We show here that Fd levels declined in tobacco (*Nicotiana tabacum*) plants exposed to oxidants or to adverse environmental conditions and that the expression of Fld in chloroplasts, but not in the cytosol, compensated for this loss and resulted in transgenic lines displaying increased tolerance to oxidative stress and to a wide range of environmental challenges. We also demonstrate that Fld is reduced in vitro by the chloroplast PETC and can provide reducing equivalents for $NADP^+$ photoreduction and Trx reduction via FTR. These activities decisively contribute to the increased stress tolerance of Fld-expressing plants by preserving the active state of redox-sensitive photosynthetic and scavenging enzymes under harmful conditions.

RESULTS

Levels of Chloroplast Fd Decline in Stressed Tobacco Plants

We first tested the effects of several adverse conditions on the leaf contents of Fd using immunoblot analysis. Exposure of 2-month-old wild-type tobacco plants (cv Petit Havana) grown in soil to MV led to a significant decrease in Fd levels (Figure 1A, wild-type lanes). Depletion of the iron–sulfur protein was also evident when plants were illuminated at low temperature or subjected to water deprivation (Figure 1A, wild-type lanes). These lower levels were not a reflection of general protein breakdown or aggregation caused by the stress situations. When leaf extracts corresponding to the same amounts of soluble protein were resolved by SDS-PAGE, similar protein profiles were obtained for all treatments and the fraction of aggregates was negligible (Figure 1C, wild-type lanes), indicating that Fd declined with respect to the bulk of stromal protein in the stressed plants.

Fld Productively Interacts with Electron Transfer Systems of Chloroplasts

The decrease of Fd levels under oxidative conditions implies the potential compromise of several Fd-dependent electron transport pathways. Consequently, the replacement of Fd by Fld and its functional engagement in chloroplast oxidoreductive pathways could be beneficial under conditions that promote Fd decline. Therefore, we evaluated whether the bacterial flavoprotein could sustain thylakoid electron transport and Trx reduction in vitro. These two Fd-dependent processes were chosen because they are involved in photosynthetic assimilation and antioxidant protection and therefore play a central role in the survival of

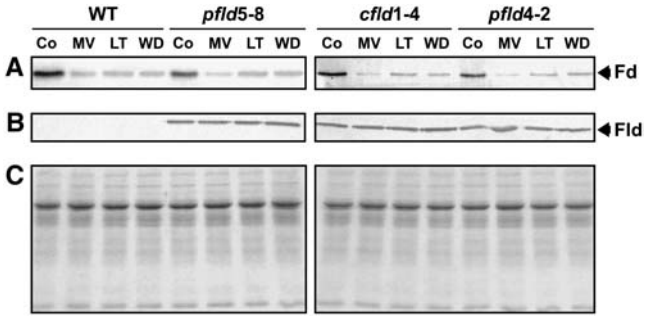

Figure 1. Fd Declines in Plants Subjected to Environmental Stress.

(A) and **(B)** Two-month-old plants grown in soil were exposed to 30 μM MV (sprayed on the aerial parts), low temperature (LT), or water deficit (WD). Growth chamber (Co) and stress conditions are detailed in Methods. Extracts were prepared from the youngest fully expanded leaves (node 8) by the freeze-clamp procedure and analyzed by SDS-PAGE and immunoblotting with Fd **(A)** or Fld **(B)** antiserum.

(C) Extracts were resolved as described above but stained for protein with Coomassie blue.

Lysates corresponding to 15 μg of soluble protein were loaded onto each lane. The positions of Fd and Fld are indicated by arrowheads.

stressed plants. Illumination of washed thylakoids in the presence of $NADP^+$ and purified *Anabaena* Fld led to steady production of NADPH (see Supplemental Figure 1 online), indicating that the flavoprotein was indeed able to interact with the chloroplast PETC in vitro. Electron transfer rates saturated at 0.94 ± 0.11 μmol NADPH·min^{-1}·mg^{-1} chlorophyll, compared with 1.73 ± 0.30 μmol NADPH·min^{-1}·mg^{-1} chlorophyll for chloroplast Fd.

Trx reduction can be determined by measuring the reductive regeneration of peroxidases of the 2-Cys peroxiredoxin (Prx) family (Collin et al., 2003). To determine whether Fld could replace Fd as the electron donor for Prx reduction, we designed a reconstituted system in which the flavoprotein was reduced in vitro via NADPH and FNR in a medium containing purified FTR, Trx *f*, and Prx. The oxidized and reduced forms of Prx can be resolved by noreducing SDS-PAGE, as oxidized Prx retains an intersubunit disulfide bond and migrates as a dimer. Prx was progressively converted into the reduced form at increasing Fld concentrations (Figure 2A), with 50% reduction ($S_{0.5}$) achieved at ~5 μM Fld (Figure 2B). Under similar conditions, plant Fd was approximately twofold more efficient (Figure 2A). Two other chloroplast Trxs, Trx *m* and Trx *x*, could also mediate this reaction, with Trx *x* being the most effective (Figure 2C). Fld was able to sustain the Trx-dependent peroxidase activity of Prx with the three Trxs (Figure 2D). Once again, the highest activities were obtained with Trx *x* (Figure 2D).

Expression of *Anabaena* Fld in Tobacco Plants

These results indicate that bacterial Fld is able to exchange electrons in vitro with plastidic Fd redox partners other than FNR. We then evaluated whether these activities could occur in the chloroplasts of living plants and contribute to survival under stress when Fd levels decline. To address this question, we generated transgenic tobacco plants expressing the flavoprotein in plastids (*pfld* lines, for plastidic flavodoxin) under the control of the cauliflower mosaic virus 35S promoter. We also prepared transgenic lines with cytosolic expression of Fld, using a construct that lacked the sequences encoding the chloroplast-targeting transit peptide. The resulting transformants were termed *cfld* (for cytosolic flavodoxin). Leaf contents of the introduced flavoprotein varied among transformed lines (see Supplemental Figure 2A online), presumably reflecting position effects during T-DNA integration. Primary transformants displaying various levels of Fld expression and containing a single transgene insertion locus per genome were self-pollinated, and homozygous plants were further selected by segregation analysis after backcrosses into the wild type. Homozygous plants displayed a proportional increase in Fld contents (see Supplemental Figure 2B online). Fld levels were maintained for several generations (see Supplemental Figure 2C online), indicating that the transgene was neither lost nor silenced during seed propagation.

Immunodetection experiments were used to confirm Fld intracellular sorting in the various transformed lines. Fld was recovered from purified chloroplasts of *pfld* plants (Figures 3A, 3C, and 3D), whereas plastids isolated from specimens transformed with the *cfld* construct contained no detectable traces of the foreign flavoprotein (Figure 3D). In *pfld* specimens, Fld distribution between total leaf and chloroplast extracts matched that of two plastid markers, Fd and the large subunit (LSU) of ribulose-1,5-bis-phosphate carboxylase/oxygenase (Rubisco), and differed from those exhibited by two cytosolic enzymes: pyrophosphate fructose 6-phosphate phosphotransferase (PFP) and NAD(H)-dependent malate dehydrogenase (NAD-MDH) (Figure 3A). Samples were analyzed by SDS-PAGE and immunoblotting on the basis of equal chlorophyll loading, rendering similar amounts of the plastidic proteins per chlorophyll in leaf and chloroplast extracts (Figure 3A), as expected for this type of component. Correct Fld sorting to the chloroplast and cytosol in *pfld* and *cfld* lines, respectively, was also revealed by immunolocalization in cross sections of young fully expanded leaves. Significant immunogold label was detected within the chloroplasts in *pfld* plants and in the cytosol of *cfld* cells (Figure 3B).

The flavoprotein was predominantly recovered (80 to 100%) as a mature-sized species in both leaf and chloroplast extracts, indicating that the transit peptide could be cleaved in vivo. This processed form was largely resistant to limited proteolysis of intact chloroplasts with thermolysin but was completely digested when the treatment was applied on osmotically ruptured organelles (Figure 3C), confirming plastid uptake and internalization. In some preparations, a slower-migrating band, differing by ~2 kD and representing a minor fraction of the entire immunoreactive product, was also detected (Figure 3C; see Supplemental Figures 2C and 2D online), presumably resulting from incomplete cleavage of the transit peptide. Indeed, thermolysin treatment of an intact *pfld* chloroplast preparation containing the two Fld forms resulted in the complete disappearance of the upper band (Figure 3C), indicating that this protein species was bound to the outer surface of the chloroplast envelope and hence exposed to the protease. The imported flavoprotein was associated, for the most part, with the stromal fraction of chloroplasts (Figure 3D).

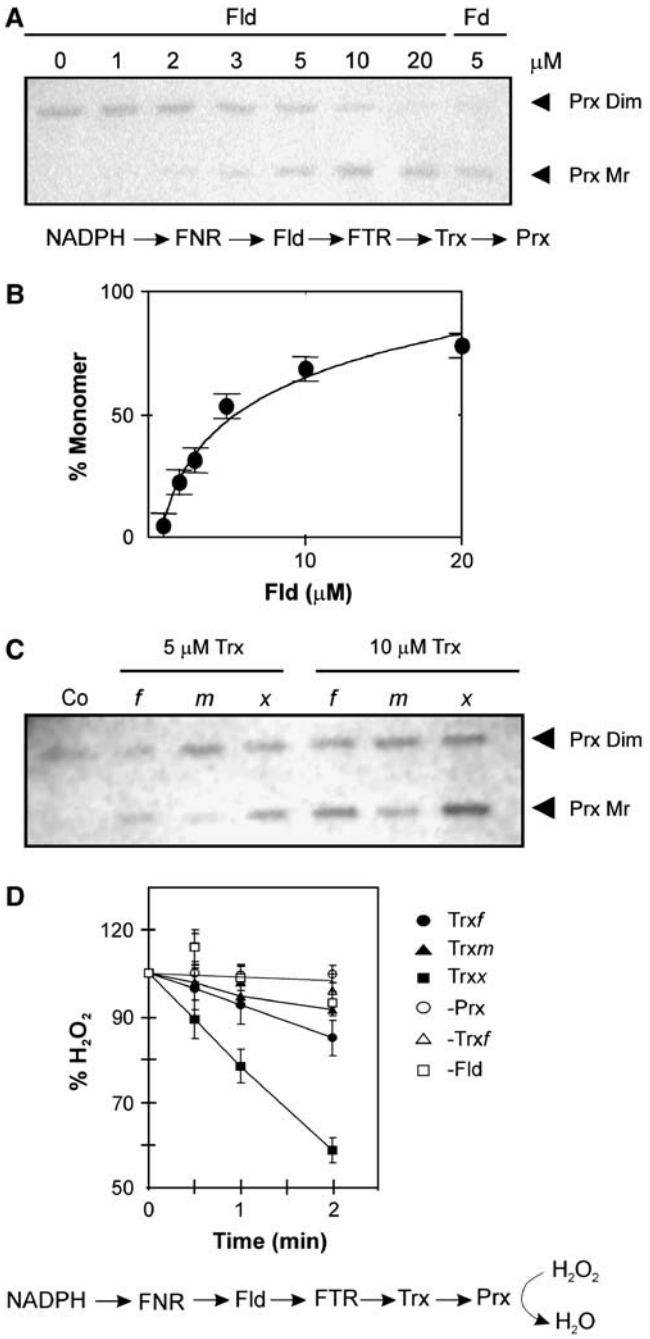

Figure 2. Fld Can Donate Electrons for Trx Reduction Mediated by Fd-Trx Reductase.

(A) In vitro reduction of purified 2-Cys Prx from *Arabidopsis* by a reconstituted electron transport chain (depicted below the gel) containing 10 μM Trx *f*. The amounts of Fld or Fd added to the reaction media are indicated above each lane. After incubation for 15 min, samples were derivatized with 10 mM *N*-ethylmaleimide, separated by nonreducing SDS-PAGE, and analyzed by immunoblotting with Prx antiserum. The positions of dimeric (Dim) and monomeric (Mr; fully reduced) Prx are shown by arrowheads.

(B) Fractions of monomer as a function of Fld concentration in the reconstituted medium. The experimental values were fit to the equation of a hyperbolic curve, with 50% reduction for Fld of 4.6 μM.

(C) Reduction of Prx by different Trxs. Experimental conditions were as described for **(A)**. Reaction media contained 10 μM Fld and were supplemented with no Trx (Co) or with 5 to 10 μM Trx *f*, *m*, or *x*, as indicated above each lane.

(D) H_2O_2 reduction by the Fld-driven reconstituted system. Reaction media contained 10 μM Trx *f* (closed circles), Trx *m* (closed triangles), or Trx *x* (closed squares). At the times indicated, the amounts of H_2O_2 remaining in the reaction media were determined by reaction with xylenol orange. Controls were assayed in the absence of Trx, Prx, or Fld (open symbols).

Plants Expressing a Cyanobacterial Fld in Chloroplasts Develop Increased Tolerance to Various Sources of Environmental Stress

Plastidic lines *pfld*5-8, *pfld*4-2, and *pfld*12-4 and cytosolic lines *cfld*1-4 and *cfld*2-1 were able to accumulate 70, 57, 7, 108, and 127 pmol of Fld per gram of leaf fresh weight, respectively, as estimated by integration of the immunoblot signals and comparison with pure standards (see Supplemental Figure 2D online). When cultured in a growth chamber (see Methods), no phenotypic differences were observed between wild-type and transgenic plants (see Supplemental Table 1 online). Photosynthetic activities also failed to reveal major changes in either maximal CO_2 assimilation rates (Figure 4C) or the light intensity at which saturation was attained (see Supplemental Table 1 online). The only significant difference among the lines was in the fluorescence quantum yield of PSII photochemistry (ϕ_{PSII}), which was 2- to 2.5-fold higher in leaf discs from *pfld*5-8 and *pfld*4-2 plants, corresponding to a doubling in the electron transport rates through PSII (Figure 4C). These ϕ_{PSII} changes did not result from increases in the capture efficiency of excitation energy by PSII, nor did they lead to overreduction of the PETC. Indeed, all lines displayed similar maximum photochemical efficiency of PSII in the dark-adapted state (F_v/F_m), chlorophyll *a*/*b* ratios (Figure 4C), and relative reduction state of PSII reflected by (1 – *qP*) values (data not shown).

In contrast with control conditions, transgenic and wild-type plants did show striking differences when assayed under stress. Six-week-old plants expressing plastid-targeted Fld survived treatment with 30 μM MV (added to the hydroponic solution), whereas wild-type and *cfld* specimens were severely damaged under the same conditions (Figure 4A). Chloroplast ultrastructure was completely disrupted in the sensitive lines but preserved in stressed *pfld* plants (Figure 4B). Accumulation of Fld in chloroplasts, but not in the cytosol, also provided protection against MV-induced ion leakage (indicative of membrane deterioration), chlorophyll degradation, and inactivation of photosynthetic activities (Figure 4C; see Supplemental Figure 3 online). Maximal CO_2 assimilation rates and PSII quantum yields decreased in both wild-type and transformed lines, but *pfld*5-8 and *pfld*4-2 plants still exhibited significantly higher values (Figure 4C). Interestingly, the F_v/F_m parameter, which is expected to decline as a consequence of accumulated photooxidative damage to PSII, was equally low (0.5 to 0.6) in all MV-treated plants, irrespective of Fld expression (Figure 4C, shaded bars). The chlorophyll *a*/*b*

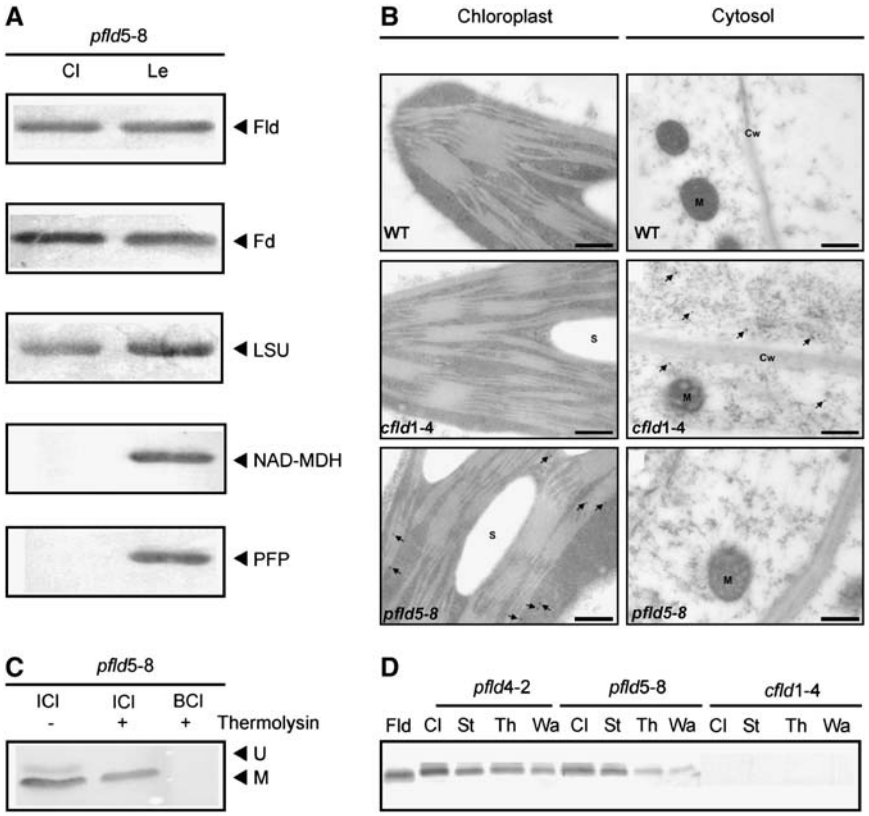

Figure 3. Subcellular Distribution of Fld in Transgenic Tobacco Plants.

(A) Fld is associated with the chloroplast fraction of *pfld*5-8 plants. Total chloroplast (Cl) and leaf (Le) extracts corresponding to 5 μg of chlorophyll were separated by SDS-PAGE on 15% acryalmide gels, blotted, and challenged with antisera specific for Fld, Fd, Rubisco LSU, NAD-MDH, or PFP.
(B) Immunolocalization of Fld in mesophyll cells of leaves from wild-type, *cfld*1-4, and *pfld*5-8 plants. Significant immunogold labeling of Fld could be detected only in chloroplasts of *pfld*5-8 and in cytosol of *cfld*1-4 leaves. Cw, cell wall; M, mitochondria; S, starch. Bars = 0.2 μm.
(C) Fld is internalized by tobacco chloroplasts in vivo. Intact chloroplasts (ICl) isolated from *pfld*5-8 specimens were resuspended in isotonic medium and incubated for 30 min on ice either in the absence (−) or presence (+) of 100 μg/mL thermolysin. The same treatment was applied to chloroplasts that had been osmotically shocked in 20 mM Tris-HCl and 1 mM EDTA (BCl). Samples corresponding to 10 μg of chlorophyll were analyzed by SDS-PAGE and immunoblotting with Fld antisera. The positions of the unprocessed (U) and mature (M) forms of the flavoprotein are indicated by arrowheads.
(D) Fld is predominantly associated with the chloroplast stroma in *pfld* plants. Chloroplasts (Cl lanes) were isolated from *pfld*4-2, *pfld*5-8, and *cfld*1-4 plants and ruptured by osmotic shock. Stromal fractions (St lanes) were cleared by centrifugation, and thylakoids (Th lanes) were washed once (Wa lanes) with rupture buffer to remove bound soluble proteins. Samples corresponding to 5 μg of chlorophyll were loaded onto each lane.
Extracts, chloroplasts, and samples for ultrastructural analysis were prepared from node-8 leaves of 8-week-old T3 plants cultured in soil under growth chamber conditions.

ratios decreased in all stressed lines, indicating loss of pigments in light-harvesting complexes and reaction centers, but this effect was less pronounced in *pfld*5-8 and *pfld*4-2 plants (Figure 4C).

Increased tolerance of Fld-expressing lines was not limited to MV toxicity. Two-week-old *pfld*5-8 and *pfld*4-2 plantlets tolerated exposure to 40°C, whereas wild-type seedlings were entirely bleached (Figure 4D; see Supplemental Figure 4A online). Similar results were obtained when the heat stress was applied on leaf discs of 2-month-old specimens grown in soil (Table 1). Transformants also exhibited increased tolerance to high light intensities, chilling, UV radiation, and water deficit (typical examples are shown in Figures 4E to 4G; see Supplemental Figures 4B to 4F online). Damage caused by all of these treatments in wild-type and *cfld* plants was reflected by extensive leaf bleaching and/or wilting (see Supplemental Figures 4A to 4F online), augmented electrolyte leakage, and declines in chlorophyll contents and photosynthetic capacities (Table 1). Tolerance of the *pfld* lines was accompanied by preservation of these functions, and in the case of plants subjected to water deprivation, by the maintenance of stomatal conductance (Table 1).

The tolerant phenotype of Fld-expressing plants was evident in assays conducted on specimens of different ages cultured on various supports (soil, agar, hydroponia), although the extent of damage and protection varied depending on the developmental stage of the plants and the growth conditions (see Supplemental Figure 4 online). In the case of MV, accessibility of the herbicide to the target tissues was also a significant factor. Visible tissue deterioration occurred faster and at lower MV concentrations

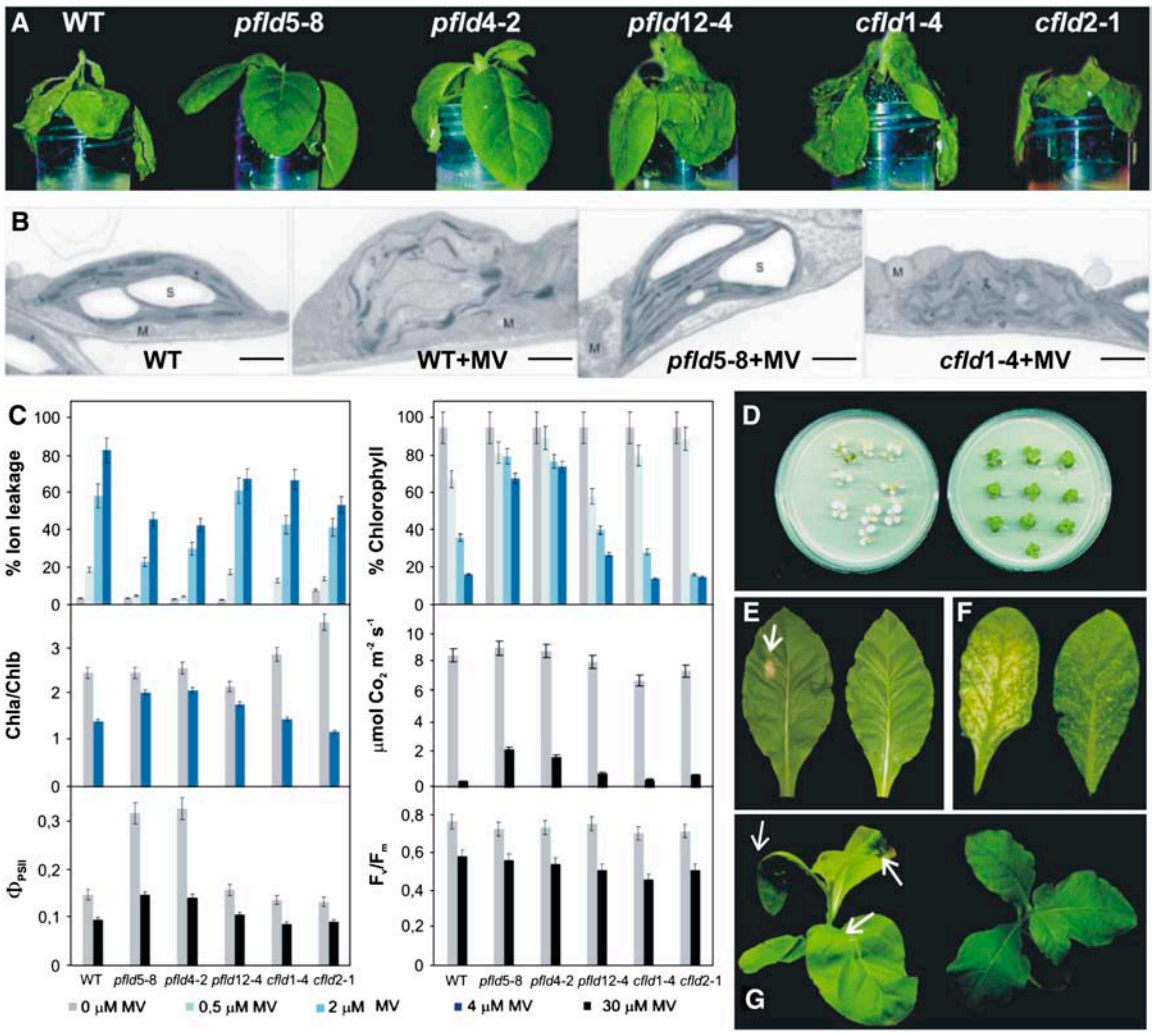

Figure 4. Fld Expression in Chloroplasts Increases Tolerance to MV and Environmental Stress Conditions.

(A) Wild-type plants and T3 transformants expressing various levels of *pfld* and *cfld* Fld were grown for 6 weeks in hydroponia and exposed for 18 h to 30 μM MV at 25°C and 500 $\mu mol \cdot m^{-2} \cdot s^{-1}$.

(B) Ultrastructural analysis of chloroplast damage in leaf cross sections of 6-week-old wild-type, *pfld*5-8, and *cfld*1-4 plants cultured in hydroponia and exposed to 30 μM MV. M, mitochondria; S, starch. Bars = 1 μm.

(C) Effect of MV treatment on membrane integrity, pigment levels, and photosynthetic activities of wild-type and transformed plants (T3 generation) grown in soil for 8 weeks. Ion leakage, chlorophyll (Chl) degradation, F_v/F_m, and ϕ_{PSII} were measured on leaf discs incubated for 18 h at 500 $\mu mol \cdot m^{-2} \cdot s^{-1}$ with the indicated concentrations of the herbicide. CO_2 assimilation rates were determined on attached leaves (node 8) from plants sprayed with 30 μM MV or Silwet. Values shown are means ± SE of four to five experiments. The chlorophyll *a* and *b* contents of each line are given in Table 1.

(D) Two-week-old seedlings from wild-type (left) and *pfld*5-8 (right) lines were illuminated for 18 h at 500 $\mu mol \cdot m^{-2} \cdot s^{-1}$ and 40°C in MS agar.

(E) Leaves from 2-month-old wild-type (left) and *pfld*5-8 (right) plants grown in soil were exposed for 18 h to a focused light beam of 2000 $\mu mol \cdot m^{-2} \cdot s^{-1}$.

(F) Seven-week-old wild-type (left) and *pfld*5-8 (right) plants were cultured for 20 d at 500 $\mu mol \cdot m^{-2} \cdot s^{-1}$ and 9°C in MS agar.

(G) Seven-week-old wild-type (left) and *pfld*5-8 (right) plants cultured in hydroponia were exposed to UV-AB radiation for 24 h.

For **(D)** to **(G)**, homozygous transformants of the T3 generation and their wild-type siblings were exposed to the stress treatments as described in Methods. The panels illustrate characteristic phenotypes, with the arrows indicating sites of tissue damage (**[E]** and **[G]**).

when the reagent was applied directly to leaves (by spraying) or floating discs than when it was fed through the roots in hydroponia (cf. the different MV sensitivities between the stressed leaves in Figure 4A and the leaf discs in Supplemental Figure 3 online). In all cases, however, there was a good correlation between stress tolerance and the levels of expressed Fld. For instance, lines *pfld*5-8 and *pfld*4-2, which are the result of distinct insertional events but accumulate similar amounts of Fld in chloroplasts, displayed equivalent levels of tolerance to MV and other sources of stress, whereas the 10-fold lower level of Fld in

Table 1. Expression of Bacterial Fld in Chloroplasts Improves the Tolerance of Transformed Tobacco Plants to Different Sources of Stress

Variable	*n*	Wild Type	*pfld*5-8	*pfld*4-2	*pfld*12-4	*cfld*1-4	*cfld*2-1
Fld contents (pmol/g fresh weight)		–	70 ± 8	57 ± 3	7 ± 3	108 ± 17	127 ± 20
Photosynthesis (μmol $CO_2 \cdot m^{-2} \cdot s^{-1}$)							
Control	8	8.7 ± 0.6	9.2 ± 0.8	9.0 ± 1.0	7.2 ± 1.2	7.1 ± 0.5	7.7 ± 1.5
UV-AB treatment	4	0.7 ± 0.1	**2.4 ± 0.1**	**2.2 ± 0.1**	0.2 ± 0.2	0.3 ± 0.1	1.1 ± 0.1
Water stress	2	0.5 ± 0.1	**6.2 ± 0.4**	**5.5 ± 0.8**	1.2 ± 0.3	1.4 ± 0.2	1.7 ± 0.5
Chlorophyll $a + b$ ($\mu g/cm^{-2}$)							
Control	24	21 ± 5	27 ± 7	24 ± 8	19 ± 11	22 ± 5	22 ± 10
High irradiation	12	14 ± 3	20 ± 3	19 ± 8	10 ± 6	15 ± 9	12 ± 4
UV-AB treatment	12	12 ± 3	**28 ± 4**	**26 ± 4**	18 ± 8	17 ± 4	18 ± 6
High temperature	12	4 ± 1	**16 ± 5**	**15 ± 9**	2 ± 1	6 ± 1	9 ± 2
Ion leakage (%)							
Control	24	5 ± 3	4 ± 1	4 ± 2	7 ± 1	8 ± 2	7 ± 1
High irradiation	12	56 ± 12	**26 ± 4**	**19 ± 7**	54 ± 8	52 ± 10	61 ± 11
UV-AB treatment	6	71 ± 10	**26 ± 9**	**30 ± 11**	79 ± 8	73 ± 16	80 ± 11
High temperature	12	81 ± 23	**32 ± 8**	**32 ± 14**	85 ± 17	80 ± 19	88 ± 9
Stomatal conductance ($mmol \cdot m^{-2} \cdot s^{-1}$)							
Control	3	281 ± 36	290 ± 46	292 ± 42	270 ± 33	273 ± 37	279 ± 45
Water stress	3	42 ± 12	**153 ± 24**	**135 ± 25**	68 ± 23	51 ± 12	51 ± 12
Survival (%)							
Control	100	99	100	98	95	98	97
30 μM MV	100	6	**66**	**49**	16	19	8
Irradiation (1200 $\mu mol \cdot m^{-2} \cdot s^{-1}$)	50	36	**80**	**88**	30	48	28
High temperature (40°C)	50	18	**98**	**88**	24	30	22

Wild-type plants and T3 transformants were grown in soil for 8 weeks in the growth chamber. Net CO_2 uptake rates and stomatal conductances were measured on node-8 leaves at 500 $\mu mol \cdot m^{-2} \cdot s^{-1}$. Stress treatments were applied on leaf discs, except for the water-deficit experiments, in which whole plants were used, under the conditions described in Methods. In experiments with leaf discs, independent plants of each line were assayed in triplicate. Survival tests were carried out on 2-week-old seedlings grown in MS agar and stressed for 18 h. Values given are averages ± SE. The term *n* indicates the number of total replicates. Values in boldface highlight cases in which differential stress tolerance was observed ($P < 0.05$).

*pfld*12-4 plants resulted in a susceptibility close to that of the wild type (Figure 4, Table 1; see Supplemental Figures 3 and 4 online). These results indicate that the tolerant phenotypes were attributable to expression of the transgene and not to the genome position where it was integrated after transformation.

The effects of MV on photosynthetic parameters (Figure 4C) indicate that components of the PETC were harmed or downregulated by the herbicide and that Fld was able to compensate for this loss, allowing substantial electron transport even under suboptimal photon capture conditions. The results shown in Figure 1A suggest that one of the missing components could be Fd. Indeed, analysis of Fd contents in transgenic lines confirmed its depletion under various stress conditions, with overall declines comparable to those of the wild-type plants (Figure 1A), whereas Fld levels were hardly affected by the treatments (Figure 1B). The collected results suggest that chloroplast Fd became limiting under stress conditions and that Fld expression was able to compensate for this loss.

Chloroplast-Targeted Fld Behaves as an Antioxidant in Stressed Transgenic Plants

The levels of H_2O_2 and superoxide were found to be equivalent in leaves of unstressed plants irrespective of Fld expression, but their buildup under adverse conditions was impaired in the lines accumulating Fld in chloroplasts, relative to wild-type and *cfld* plants (Figure 5). A similar trend was observed when measuring the formation of malondialdehyde (MDA), a proxy for membrane lipid peroxidation (Figure 5), indicating that the tolerance of Fld-expressing lines correlated with a decrease in ROS accumulation. Of the oxidants assayed, superoxide determination is less reliable because of the limited life span of this radical in living tissues. Even though its absolute contents should be considered with caution, differences between the various stressed lines were highly significant ($P < 0.05$).

Protection was not mediated by a general induction of the antioxidant capacity in the host cell. Under normal growth conditions, the total activities of superoxide dismutase (SOD), ascorbate peroxidase (APX), and glutathione reductase (GR) were similar in total leaf extracts obtained from control and transgenic plants (see Supplemental Table 2 online). The patterns of leaf-associated SOD and APX isoforms, resolved by nondenaturing PAGE, also failed to reveal significant differences (even in minor isoenzymes) among the various lines (see Supplemental Figure 5 online). Moreover, we did not detect significant induction of any of these protective systems after 12 h of MV treatment (see Supplemental Table 2 online). Immunoblot detection of some components of the FTR/Trx pathway (Trx *f*, Trx *m*, and FTR) revealed that their levels were hardly affected by either Fld expression or oxidative stress (see Supplemental Figure 6 online). Similar results have been obtained by microarray analysis of *Arabidopsis* plants exposed to various environmental hardships (Zimmermann et al., 2004).

The total pool of ascorbate species, represented by the sum of ascorbic acid (ASC) and dehydroascorbic acid (DHA), displayed

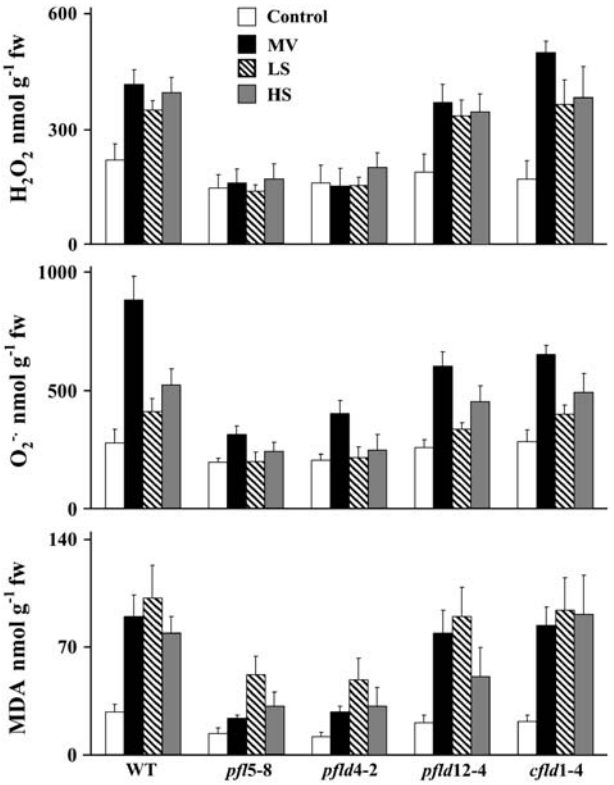

Figure 5. Effect of Fld Expression on the Levels of Oxidants in Plants Exposed to Various Sources of Stress.

Assays were conducted in leaf extracts from soil-cultured 2-month-old transgenic plants (T5 generation) and their wild-type siblings. Leaves from node 9 were incubated under growth chamber conditions (open bars) or exposed to 30 μM MV at 500 $\mu mol \cdot m^{-2} \cdot s^{-1}$ (closed bars), to light stress (LS) at 1200 $\mu mol \cdot m^{-2} \cdot s^{-1}$ (hatched bars), or to heat stress (HS) at 40°C (shaded bars). Exposure times were 18 h in all cases. Methods used to estimate ROS and MDA levels are detailed in Methods. Data shown are averages ± SE of five experiments. Values reported for *pfld*5-8 and *pfld*4-2 differed significantly from those of the other lines ($P < 0.05$). fw, fresh weight.

similar levels in leaves from unstressed plants of all lines assayed (see Supplemental Table 2 online). This pool experienced a mild decrease (~20%) after treatment with MV, but ASC oxidation was partially prevented in the tolerant *pfld* specimens (Figure 6; see Supplemental Table 2 online for actual contents). In the absence of stress, the levels of GSSG were significantly lower in leaves of *pfld*5-8 and *pfld*4-2 plants, resulting in higher GSH:GSSG ratios, and this trend was maintained after MV application (Figure 6; see Supplemental Table 2 online for actual contents).

Fld Supplies Electrons to Trx Reductive Pathways in Chloroplasts

Purified Fld was able to sustain Prx regeneration mediated by the Trx/FTR system in vitro (Figure 2). Therefore, we investigated whether this Fld activity could have any effect on Prx turnover in vivo. When ROS concentrations increase to toxic levels, as occurs under stress conditions, Prx can be overoxidized and inactivated (Wood et al., 2003). This Prx form also dissociates under denaturing conditions (König et al., 2002; Broin and Rey, 2003). We observed an increase in overoxidized Prx when wild-type or *cfld*1-4 plants were exposed to MV, water deficit, or cold treatments (Figure 7A; see Supplemental Table 3 online). By contrast, the amount of the presumably overoxidized monomer was significantly lower in leaves from plants expressing Fld in chloroplasts and subjected to the same treatments (Figure 7A; see Supplemental Table 3 online).

Because both the fully reduced and overoxidized forms of 2-Cys Prx behave as noncovalently bound dimers that break up into monomers during nonreducing SDS-PAGE (Figure 7B), we further characterized the species obtained under the two conditions by two-dimensional gel electrophoresis. Overoxidized Prx was first separated from the disulfide-linked dimer and the fully reduced species by isoelectric focusing, taking advantage of the additional negative charge introduced by the sulfinic acid group formed during overoxidation (Wood et al., 2003). Samples were then reduced with DTT, subjected to a second dimension SDS-PAGE, and analyzed by immunoblotting with Prx antisera. The purified enzyme was identified as a distinct spot (pI ~ 5.4) on the two-dimensional gels, before or after reduction by the

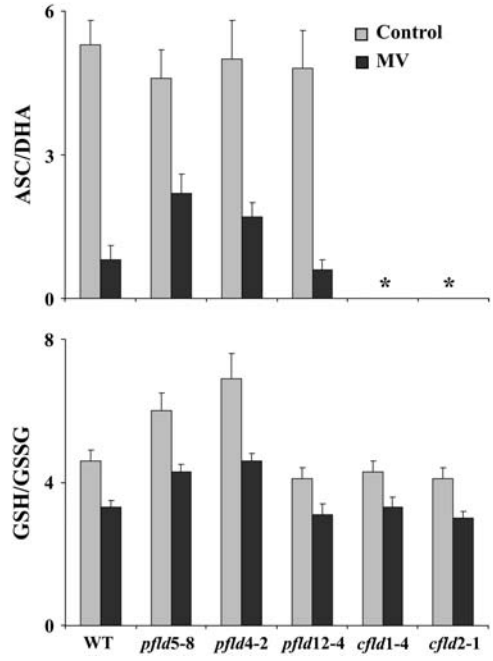

Figure 6. Effect of Fld Expression on the Levels of Antioxidant Metabolites in Plants Exposed to MV.

Assays were conducted in leaf extracts from soil-cultured 2-month-old wild-type and transgenic plants (T5 generation) sprayed (closed bars) or not (gray bars) with 30 μM MV. Levels of ASC, DHA, GSH, and GSSG were estimated according to published procedures (Foyer et al., 1995). Means ± SE of three experiments are shown. Values reported for *pfld*5-8 and *pfld*4-2 differed significantly from those of the other lines ($P < 0.05$). Asterisks indicate values not determined.

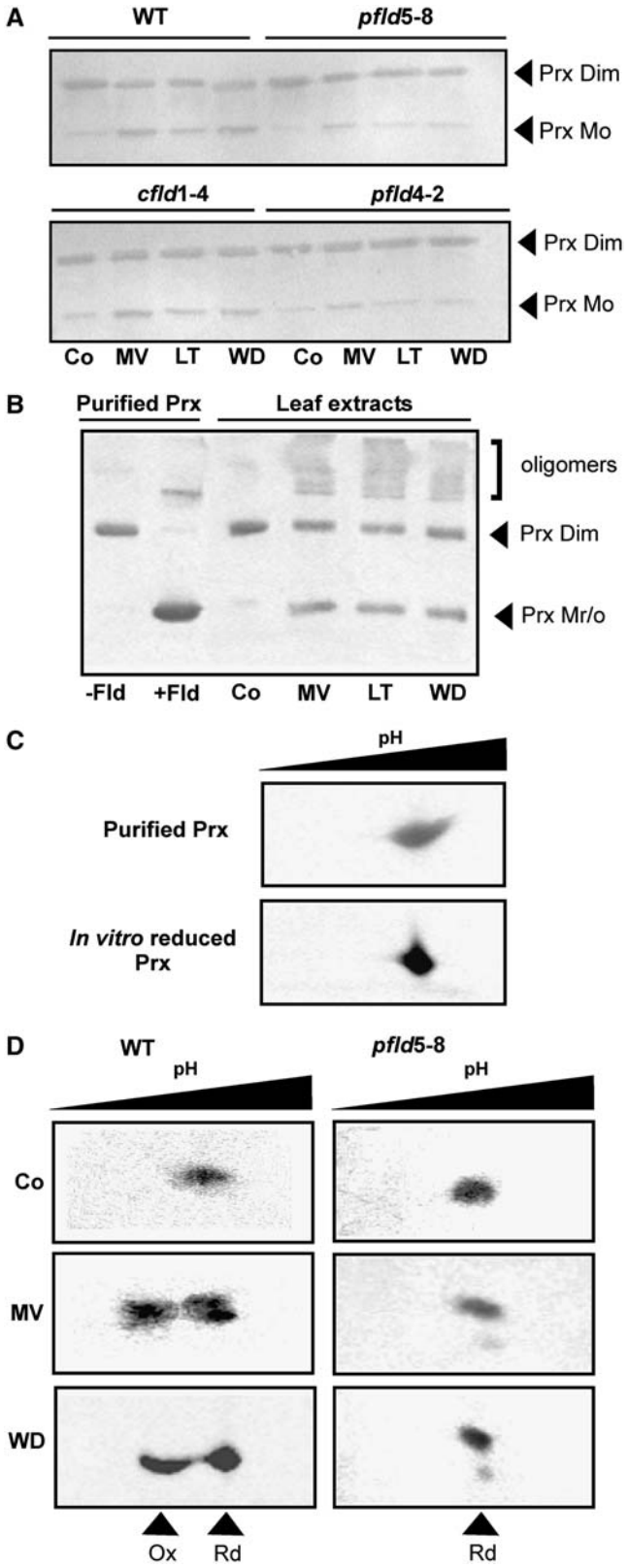

Figure 7. Fld Expression Modulates the Redox State of Chloroplast 2-Cys Prx in Stressed Plants.

Fld-containing reconstituted system (Figure 7C). A single immunoreactive signal could also be recognized on two-dimensional gels of leaf extracts from unstressed wild-type or *pfld*5-8 specimens (Figure 7D). After exposure of wild-type plants to MV or water deficit, satellite spots appeared at more acidic positions at the expense of the original signals, consistent with the conversion of Prx to the sulfinic acid form (Figure 7D). Little or no overoxidized Prx could be detected in leaf extracts from stressed *pfld*5-8 (Figure 7D) or *pfld*4-2 plants (data not shown), indicating that Fld accumulation in chloroplasts was able to keep higher amounts of Prx in the productive peroxidatic cycle.

Prxs are not the only Fd/Trx targets in chloroplasts, raising the possibility that other subjects of reductive modulation could also be protected from oxidative inactivation in Fld-containing plants. Accordingly, we observed that the activation state of the chloroplast NADP(H)-dependent malate dehydrogenase (NADP-MDH) was largely preserved in *pfld*5-8 and *pfld*4-2 plants subjected to water deficit or MV toxicity, whereas it declined significantly in wild-type and *cfld*1-4 siblings (Figure 8; see Supplemental Table 3 online for specific activities). Target enzymes of central metabolic pathways, such as the Calvin cycle components fructose-1,6-bisphosphatase (FBPase) and phosphoribulokinase (PRK), were also protected from oxidative inactivation in stressed plants expressing Fld in plastids (Figure 8; see Supplemental Table 3 online for specific activities).

DISCUSSION

Fd plays a key role in the physiology of the plant cell, and alterations of its levels are expected to have pleiotropic effects, because multiple essential metabolic and signaling processes depend upon reduction by this iron–sulfur protein. The amounts

(A) Fld accumulation in chloroplasts prevents the oxidation of 2-Cys Prx in plants subjected to environmental stress. Wild-type, *pfld*5-8, *cfld*1-4, and *pfld*4-2 specimens were grown in soil for 8 weeks and then exposed to 30 μM MV, low temperature (LT), or water deficit (WD) as described in Methods. Controls (Co) were incubated under growth chamber conditions for the same periods. Extracts were prepared from young leaves corresponding to node 8 by the freeze-clamp procedure, and samples corresponding to 8 μg of soluble protein were analyzed by nonreducing SDS-PAGE and immunoblotting. The positions of dimeric (Dim) and monomeric (Mo; overoxidized) Prx are shown by arrowheads.

(B) Electrophoretic mobility of fully reduced and overoxidized Prx monomers. In vitro reduction of purified Prx was performed with the reconstituted system containing (+) or not (−) 10 μM Fld, essentially as described for Figure 2, except that the reaction was prolonged for 60 min. Stress treatments (MV, LT, WD) were applied as indicated for **(A)**, and leaf extracts corresponding to 16 μg of total soluble protein were analyzed by SDS-PAGE and immunoblotting. *N*-ethylmaleimide derivatization was omitted, resulting in the accumulation of aggregates, as reported previously (König et al., 2002). Mr, fully reduced.

(C) and **(D)** Discrimination between fully reduced and overoxidized Prx monomers. In vitro reduction of Prx **(C)** and stress treatments **(D)** were performed essentially as described for **(A)** and **(B)**. After two-dimensional SDS-PAGE, Prx spots were visualized by immunoblotting. The arrowheads indicate the positions of overoxidized (Ox) and reduced (Rd; a mixture of disulfide and dithiol forms) Prx.

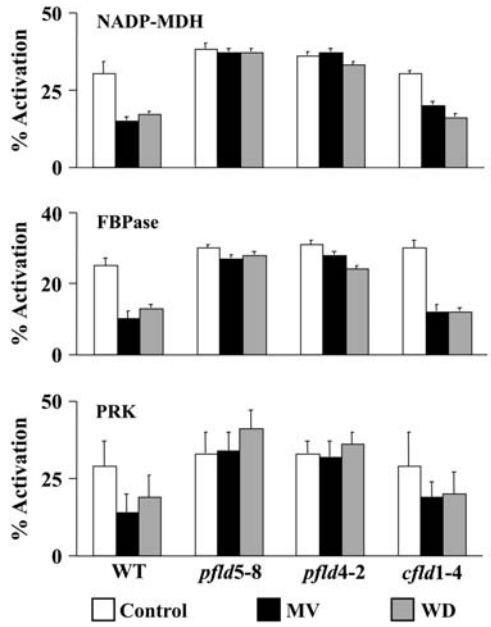

Figure 8. Activation States of Trx-Dependent Chloroplast Enzymes Are Preserved in Stressed Plants Expressing Plastid-Targeted Fld.

Two-month-old wild-type plants and T5 transformants were sprayed with 30 μM MV (closed bars), exposed to water deficit (WD; shaded bars), or incubated under growth chamber conditions for the same periods (Control; open bars). Extracts were prepared from node-8 leaves as described in Methods. The activities of NADP-MDH, FBPase, and PRK were measured before (in vivo activity) and after reduction of the extracts with DTT (total activity). The activation states were calculated as the ratio between the in vivo and total activities for each condition. Means ± SE of three to five experiments are shown. Specific activities used for the calculations and statistical differences can be found in Supplemental Table 3 online.

of Fd are known to decline in photosynthetic microorganisms in response to environmental stresses (Mazouni et al., 2003; Singh et al., 2004). Results presented in Figure 1 indicate that chloroplast Fd also decreases in plants exposed to environmental adversities. The mechanisms underlying this effect are unknown at present. Destruction of the iron–sulfur clusters by ROS could be the direct cause, but microarray analysis of the *Arabidopsis* genome indicated that Fd transcript levels declined in stressed plants (Zimmermann et al., 2004), suggesting that transcriptional and/or posttranscriptional mechanisms also might be involved in the observed decrease. Petracek et al. (1998) (and references therein) have shown that Fd expression is downregulated by a posttranscriptional mechanism when the intersystem components of the PETC become overreduced, a common condition in plants exposed to adverse environments (Allen, 1995; Apel and Hirt, 2004).

The effects of Fd deprivation on plant physiology can be fully appreciated by analyzing the phenotypes of transgenic potato lines in which the levels of this iron–sulfur electron carrier were decreased by an antisense approach (Holtgrefe et al., 2003). When the Fd contents were between 50 and 80% of those found in wild-type plants, chlorophyll was progressively lost in a dynamic process and leaves turned yellowish with increasing age. In short-term experiments, the antisense lines experienced a significant decrease in CO_2 assimilation rates, the intersystem chain components were overreduced, and the distribution of electrons toward stromal acceptors was deeply perturbed, resulting in lower levels of Trx reduction (Holtgrefe et al., 2003). Depending on the amount of remaining Fd, severely depleted lines showed photoinhibition.

Even though Fld-encoding genes were lost during the transition from algae to plants, we were able to demonstrate that incorporation of a bacterial Fld into tobacco chloroplasts could compensate for the decline in Fd levels, leading to increased tolerance to oxidants and to a wide range of adverse conditions (Figure 4, Table 1; see Supplemental Figures 3 and 4 online). The plastid-targeted flavoprotein exhibited antioxidant activity in stressed transformants, reflected by lower ROS accumulation (Figure 5) and reduced oxidative damage to sensitive enzymes (Figures 7 and 8), membranes, pigments, and photosynthesis (Figure 4, Table 1). These effects can be accounted for by Fld involvement in $NADP^+$ photoreduction (see Supplemental Figure 1 online) and especially in Trx reduction as a substrate of FTR (Figures 2 and 7). Maintenance of high levels of reduced Trx could favor a number of dissipative and scavenging pathways, including (1) Prx regeneration to eliminate H_2O_2 and organic peroxides formed under stress (Figures 2 and 7), (2) export of the excess of reducing power via the malate valve (Figure 8), and (3) productive consumption of the NADPH surplus by the Calvin cycle (Figure 8). In addition, the ascorbate and glutathione pools were maintained at a more reduced state in *pfld* lines, in the latter case even in nonstressed plants (Figure 6). One of the chloroplast routes for ASC regeneration involves Fd, and it is possible that Fld can drive this reaction in vivo, although higher ASC reduction levels could also be a secondary consequence of Prx activity preservation in these lines. Antisense suppression of Prx is reported to cause extensive oxidation of the ascorbate pool in *Arabidopsis* (Baier et al., 2000). By contrast, the link between Fld expression in chloroplasts and glutathione reduction is unclear, because GSH formation does not require Fd. It is conceivable that this effect did not stem from an increase in glutathione reduction but from a decline in GSH oxidation attributable to lower ROS accumulation in Fld-expressing transformants (Figure 5).

Still other protective routes that require a steady provision of reduced Trx, such as the oxidative pentose phosphate pathway, ATP synthesis, and redox-modulated communication of the chloroplast with the nucleus and mitochondria (Balmer et al., 2003, 2004), could also be preserved in Fld-expressing plants, but support for this contention requires rigorous experimental proof. However, many features of the tolerance exhibited by the transformants suggest a prominent role for Fld in Trx metabolism and are consistent with the reported role of 2-Cys Prxs as floodgates that scavenge oxidants only above a certain threshold, preventing toxicity but allowing their involvement in signal transduction (Wood et al., 2003). The wild-type phenotypes (Table 1; see Supplemental Table 1 online) and ROS levels (Figure 5) displayed by unstressed transformants strongly suggest that the signaling functions played by stable oxidants were not affected by Fld accumulation. A comprehensive scheme of chloroplast

Trx-dependent routes that might be subject to Fld stimulation is provided in Figure 9.

Fld behaved as an alternative intermediate for the PETC in vivo, as indicated by the increases in ϕ_{PSII} photochemistry exhibited by tolerant plants (Figure 4; see Supplemental Table 1 online). Under normal growth conditions, the excess of reducing equivalents generated in the PETC was delivered for the most part to alternative routes, and photosynthetic carbon assimilation remained unaltered (Table 1; see Supplemental Table 1 online). When plants were exposed to adverse conditions and Fd levels declined, the presence of Fld in chloroplasts permitted considerable photosynthetic rates compared with wild-type siblings (Figure 4, Table 1). It might be argued that Fld activity in $NADP^+$ photoreduction could lead to a more pronounced $NADP^+$

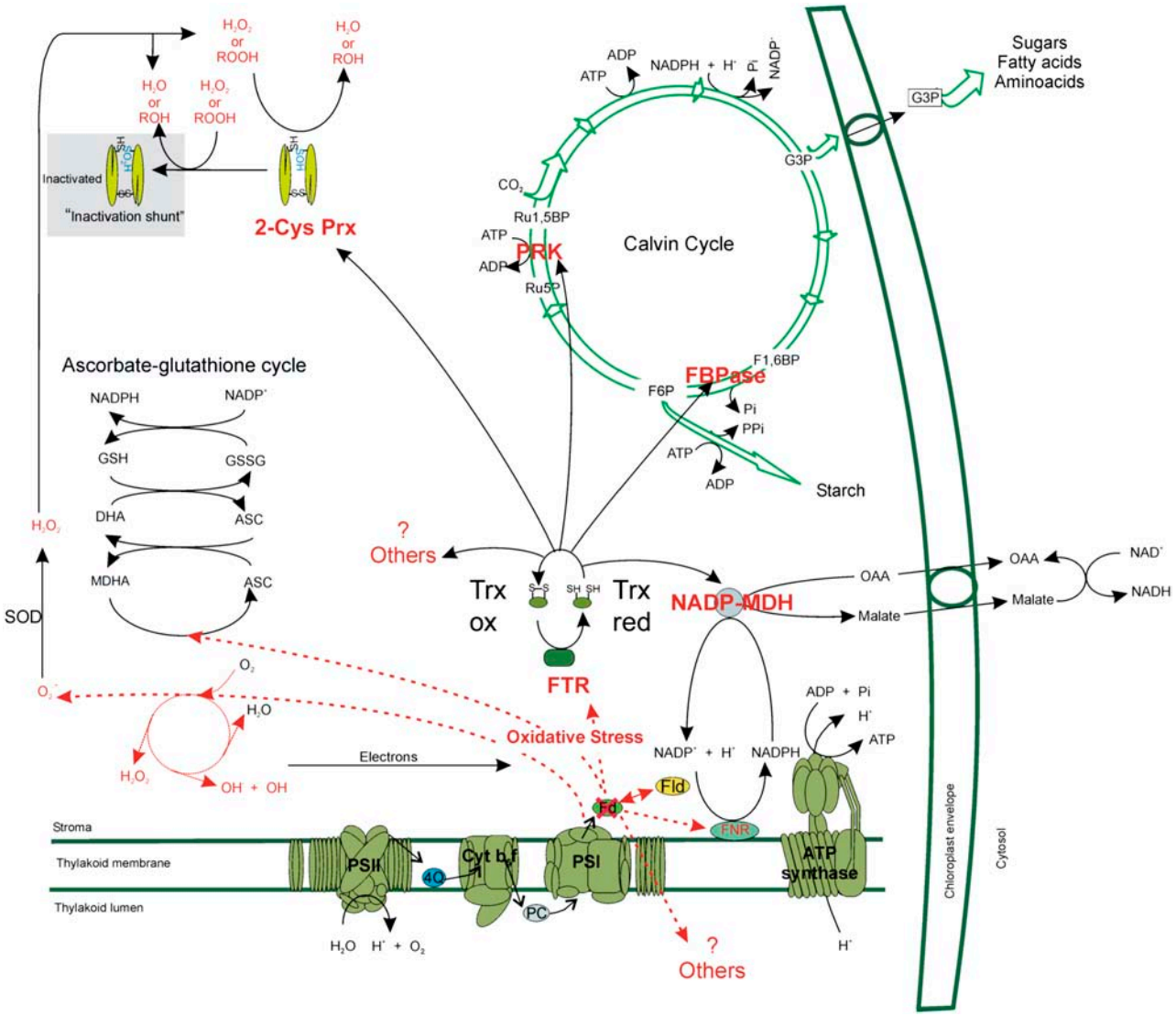

Figure 9. Model for the Protective Mechanism of Fld in Chloroplasts.

The electrons originating in the electron transport chain may be transferred from Fd or Fld to the Trx system via FTR. Trxs will then regenerate the active forms of key target enzymes (Prx, NADP-MDH, FBPase, PRK) through reduction of their critical Cys residues, resulting in the maintenance and/or stimulation of the Calvin cycle, the Prx cycle, the malate valve, and presumably other metabolic routes. Other Fd redox partners, such as FNR and the ascorbate regeneration cycle, are also shown. Fld expression is inconsequential in phenotypic terms for plants grown under normal conditions but becomes critical as Fd declines to limiting levels in the stressed organism. ASC, ascorbate; Cyt, cytochrome; DHA, dehydroascorbate; FBPase, fructose-1,6-bisphosphatase; F1,6BP, fructose-1,6-bisphosphate; F6P, fructose 6-phosphate; G3P, glyceraldehyde 3-phosphate; GSH and GSSG, reduced and oxidized glutathione; MDHA, monodehydroascorbate; NADP-MDH, NADP(H)-dependent malate dehydrogenase; OAA, oxalacetic acid; PC, plastocyanin; PRK, phosphoribulokinase; PSI and PSII, photosystems I and II; 4Q, plastoquinone; R5P, ribulose 5-phosphate; R1,5BP, ribulose-1,5-bisphosphate; SOD, superoxide dismutase.

shortage under the worse possible conditions. However, Fld also stimulated NADPH consumption by activated NADP-MDH and the Calvin cycle, providing a larger electron sink during stress. The combined effects will favor electron distribution to productive routes normally switched off or slowed down under stress and delivery of the surplus of reducing equivalents to the cytosol via the malate valve (Scheibe, 2004). These activities will prevent excessive reduction of the PETC, eliminating one of the major causes of ROS propagation, and will contribute to the healthy physiological condition exhibited by the transformed plants. They will also maintain ATP synthesis and the transmembrane proton gradient that triggers still other protective devices, such as the xanthophyll cycle (Holt et al., 2004).

Fld engagement in the Fd/Trx route, which is so prominent in chloroplasts, explains why plastid targeting was a mandatory feature for the manifestation of the protective effects observed. A similar role in the cytosol would be unlikely because the corresponding Trx reductases specifically use NADPH as the hydride donor to reduce *h*-type Trxs (Buchanan et al., 2002). The pleiotropic nature of the protection afforded concurs with the many different regulatory roles played by Trxs in the context of the chloroplast and the plant cell (Figure 9) and highlights the relevance of the Trx/FTR system for the development of the tolerant phenotypes.

It is conceivable that Fld could also interact with Fd-based pathways other than $NADP^+$ or Trx reduction. Stimulation of amino acid and fatty acid synthesis, nitrogen and sulfur assimilation, and especially ascorbate regeneration (Figure 9) as well as the dissipative routes of cyclic electron flow and chlororespiration also might contribute to the stress tolerance observed in the transformants. Hagemann et al. (1999) have demonstrated that Fld accumulation critically contributes to enhanced cyclic electron transport around PSI in stressed cells of the cyanobacterium *Synechocystis*. The possibility that Fld could replace Fd in any of these chloroplast-based pathways has not been addressed experimentally and certainly deserves further research.

The approach explored in this work was to express Fld, the gene product from a photosynthetic prokaryote, in a higher plant, where it can engage in a multiplicity of reactions affecting general plant function. Within this context, Fld manipulation could provide fresh and powerful resources to investigate the requirements of photosynthesis in vivo, based on the use of a bacterial protein whose expression is free from the endogenous regulation and feedback loops that might complicate phenotype interpretation. The proposed strategy might still benefit from the functional complementation of Fd-deficient mutant or antisense plants. Plant life appeared to be irreversibly compromised when Fd protein contents were diminished below ~50% of those present in nontransformed wild-type siblings (Holtgrefe et al., 2003). Fld expression could help to overcome this lower limit, potentially leading to the generation of transformed lines that could survive and develop with marginal levels of the iron–sulfur protein. Experiments aimed at this goal are currently under way. Finally, the broad-range stress tolerance displayed by Fld-expressing plants suggests that the use of this flavoprotein might have applications as a biotechnological tool to improve the field performance of crops grown in suboptimal environments.

METHODS

Construction of Fld Expression Vectors and Tobacco Transformation

A DNA fragment encoding *Anabaena* PCC 7119 Fld was obtained by PCR amplification of a previously isolated gene (Fillat et al., 1991) with primers 5′-GACGAGCTCTCATAATGTCAAAG-3′ and 5′-ACTGTCGACTTTTTACAAACCAAAT-3′, containing *Sac*I and *Sal*I recognition sites, respectively. Underlined bases represent the initial and termination codons of the Fld gene. The amplified fragment was digested with the corresponding enzymes and ligated in-frame to the *Sac*I end of a *Bam*HI/*Sac*I DNA, encoding the chloroplast-targeting transit peptide of pea (*Pisum sativum*) FNR (Serra et al., 1995). The fused gene was cloned between the cauliflower mosaic virus 35S promoter and polyadenylation regions of pDH51 (Pietrzak et al., 1986) to yield *pfld*. Fld DNA was also amplified using the same 3′ end primer and the oligonucleotide 5′-AAGATCAGGATCCATAATGTCAAA-3′, containing a *Bam*HI site, as the 5′ end primer. The PCR fragment was digested with *Bam*HI/*Sal*I and cloned in pDH51 to produce *cfld*. Both constructs (*pfld* and *cfld*, directing Fld expression to plastids and the cytosol, respectively) were excised from pDH51 plasmids with *Eco*RI and inserted into compatible sites of the binary vector pCAMBIA 2200 (Hajdukiewicz et al., 1994). Recombinant plasmids were introduced into the genome of tobacco (*Nicotiana tabacum* cv Petit Havana) through *Agrobacterium tumefaciens*–mediated leaf disc transformation (Gallois and Marinho, 1995).

Homozygous lines were selected by following kanamycin resistance and Fld levels in the progeny of self-pollinated primary transformants. The presence of the bacterial flavoprotein in cleared leaf extracts was analyzed by SDS-PAGE on 15% polyacrylamide gels, followed by immunoblot analysis with Fld antisera. Reactive bands were integrated using the Multi-Analyst Package 1.1 from Bio-Rad, and Fld contents were estimated by comparison with pure standards (see Supplemental Figure 2D online). The concentration of the purified protein was determined by the absorption of bound flavin mononucleotide, using $\varepsilon_{454} = 8.8\ mM^{-1}\ cm^{-1}$.

Plant Growth and Characterization

Seeds were germinated on Murashige and Skoog (MS) agar plates supplemented with 2% (w/v) sucrose and, in the case of transformants, 100 μg/mL kanamycin. After 4 weeks, seedlings were transferred to new MS agar or soil or grown hydroponically in nutrient medium (Geiger et al., 1999). Soil-cultured plants were watered daily with the same solution and illuminated in all cases at 200 $\mu mol \cdot m^{-2} \cdot s^{-1}$ and 25°C to provide a 14-h photoperiod (growth chamber conditions).

Stress treatments were performed with homozygous plants belonging to various generations (T3 to T6). Plants transferred to hydroponia were cultured for 2 to 4 weeks before exposure to adverse conditions. Most experiments were performed with specimens grown in soil for 8 to 9 weeks. These plants usually contained 10 to 11 nodes with internodal distances of 6 to 7 cm (Table 1). Treatments were performed on whole plants or on the youngest fully developed leaves, corresponding to nodes 8 or 9 (counting from the bottom) of wild-type and transformed specimens. To improve reproducibility and facilitate comparisons between lines, we always assayed, side-by-side, tissues of the same developmental stage (the same node) in wild-type and transformed plants that displayed similar height and number of nodes. Statistical analysis was conducted using a two-sided *t* test.

Plants were exposed to MV by spraying the aerial parts or through the nutrient solution, depending on whether they were cultured in soil or hydroponia, respectively. The spraying solution contained 0.005% (v/v) Silwet. Discs (12 mm diameter) were punched from expanded leaves (nodes 8 to 9) of 2-month-old plants grown in soil and floated topside

up in 1 mL of water or MV. Plants and discs were illuminated at 500 $\mu mol \cdot m^{-2} \cdot s^{-1}$ for 18 h, unless stated otherwise, whereas controls were kept in the dark. Ion leakage was measured as the increase in conductance of the medium using a Horiba B-173 conductivity meter. At the end of the assay, samples were autoclaved to disrupt all cells, and total electrolyte contents were determined in the resulting solution.

To evaluate the tolerance to high temperatures, 2-week-old seedlings cultured in MS agar or leaf discs from 2-month-old plants grown in soil were exposed to 500 $\mu mol \cdot m^{-2} \cdot s^{-1}$ at 40°C for 12 h on MS agar plates. Chilling sensitivity was assayed in 7-week-old plants grown in MS agar that were cultured for 20 d at 9°C and 500 $\mu mol \cdot m^{-2} \cdot s^{-1}$ or in 2-month-old plants grown in soil and exposed to 4°C and 500 $\mu mol \cdot m^{-2} \cdot s^{-1}$ for 48 h. Treatments with intense illumination were performed in 2-month-old plants grown in soil by focusing a light beam of 2000 $\mu mol \cdot m^{-2} \cdot s^{-1}$ for 18 h at 25°C on the upper surface of a fully expanded leaf from node 8 with the aid of a light cannon. Plants of similar age were also subjected to a 3-d water deficit regime or to UV-C radiation. In the latter case, samples were exposed to a germicidal lamp (Phillips 36 W/636T8) placed at 60 cm in a laminar flow hood (CASIBA HI3) for 20 min and photographed after 3 d. Tolerance to UV-AB radiation was assayed by exposing 6-week-old plants cultured in hydroponia to a combination of UV-A (315 to 380 nm, 2.2 W/m^2) and UV-B (280 to 315 nm, 1.0 W/m^2) radiation for 24 h at 25°C. Leaf discs from 2-month-old plants grown in soil were also subjected to heating, high light intensity (1200 $\mu mol \cdot m^{-2} \cdot s^{-1}$), and UV-AB radiation essentially as described above, except that treatments were applied for 18 h in these cases.

Fixation, Substitution, and Embedding for Light and Transmission Electron Microscopy

For the primary fixation, 1-mm^2 sections of leaf tissue were incubated for 2.5 h at 25°C in 50 mM cacodylate buffer, pH 7.2, containing 0.5% (v/v) glutaraldehyde and 2.0% (v/v) formaldehyde, followed by one wash with buffer and two washes with distilled water. Samples for immunogold labeling studies were dehydrated stepwise by increasing the concentration of ethanol under progressive lowering of temperature in an automated freeze substitution unit (AFS; Leica). The steps used were as follows: 30% (v/v), 40% (v/v), and 50% (v/v) ethanol for 1 h each at 4°C; 60% (v/v) and 75% (v/v) ethanol for 1 h each at −15°C; 90% (v/v) ethanol and twice 100% (v/v) ethanol for 1 h each at −35°C. The samples were subsequently infiltrated with Lowycryl HM 20 resin (Plano) by incubating them in the following mixtures: 33% (v/v), 50% (v/v), and 66% (v/v) HM 20 resin in ethanol for 4 h each and then 100% (v/v) HM 20 resin overnight. Samples were transferred into gelatin capsules, incubated for 3 h in fresh resin, and polymerized at 35°C for 3 d under indirect UV light. Thin sections, 70 nm thick, were cut with a diamond knife and used for immunogold labeling with anti-Fld as the primary antibody and 10 nM protein A–gold as described by Teige et al. (1998).

Samples for ultrastructural analysis and light microscopy were transferred after primary fixation into a solution of 1% (w/v) OsO_4 for secondary fixation. After 1 h, samples were washed three times with distilled water. Dehydration at 25°C was performed stepwise by increasing the concentration of ethanol as follows: 30% (v/v), 50% (v/v), 60% (v/v), 75% (v/v), 90% (v/v), and twice 100% (v/v) ethanol for 1 h each. After additional dehydration with propylene oxide for 1 h, the samples were infiltrated with Spurr resin (Plano) as follows: 33% (v/v), 50% (v/v), and 66% (v/v) Spurr resin in propylene oxide for 4 h each and then 100% (v/v) Spurr resin overnight. Samples were transferred into embedding molds, incubated there for 3 h in fresh resin, and polymerized at 70°C for 24 h. Semithin sections with a thickness of ~3 μm were mounted on slides and stained for 2 min with 1% (w/v) methylene blue and 1% (w/v) Azur II in 1% (w/v) aqueous borax at 60°C before light microscopic examination. For electron microscopic analysis with a Zeiss CEM 920A transmission electron microscope at 80 kV, ultrathin sections with a thickness of ~70 nm were cut with a diamond knife and contrasted with a saturated methanolic solution of uranyl acetate and lead citrate before examination.

Activity Determinations

Light-dependent CO_2 assimilation and stomatal conductance were determined on attached leaves from nodes 8 or 9 of 2-month-old plants grown in soil using an LI-6200 portable photosynthesis system from Li-Cor. The CO_2 concentration of the air entering the leaf chamber and the temperature were adjusted to 360 ppm and 20°C, respectively. PPFD ranging from 50 to 1000 $\mu mol \cdot m^{-2} \cdot s^{-1}$ was supplied by a controlled halogen light source. Chlorophyll *a* fluorescence measurements were performed at 25°C on dark-adapted leaves of the same plants using a Qubit Systems pulse-modulated fluorometer. The F_v and F_m parameters were determined after 30 min in the dark, and the light-adapted values (F_v' and F_m') were measured after 30 min of illumination with 500 $\mu mol \cdot m^{-2} \cdot s^{-1}$. Photosynthetic parameters (F_v/F_m, ϕ_{PSII}, and nonphotochemical and photochemical quenching) were calculated as described (Baker and Rosenqvist, 2004).

$NADP^+$ photoreduction, using water as the electron donor, was measured at 25°C in 3 mL of 50 mM HEPES-KOH, pH 8.0, 5 mM $MgCl_2$, 330 mM sorbitol, 0.5 mM $NADP^+$, thylakoids corresponding to 20 μg of chlorophyll, and 20 μM Fld. Illumination (2400 $\mu mol \cdot m^{-2} \cdot s^{-1}$) was provided by a projector lamp, and the amount of NADPH formed was estimated by measuring the increase in absorption at 340 nm ($\varepsilon_{340} = 6.2\ mM^{-1}\ cm^{-1}$).

SOD, APX, and GR were extracted from leaf tissue using the conditions and homogenization solutions reported by Gupta et al. (1993). Procedures used to assay their activities are also described there. The patterns of SOD and APX isoenzymes were analyzed by resolving cleared extracts corresponding to 45 and 170 mm^2 of leaf tissue, respectively, by nondenaturing PAGE and activity staining (Beauchamp and Fridovich, 1971; Mittler and Zilinskas, 1993).

Samples used for the estimation of the in vivo enzymatic activities of chloroplast NADP-MDH, FBPase, and PRK were prepared by the freeze-clamp method. At the end of the treatment or illumination periods, young leaves from node 8 of both control and transgenic plants grown in soil were harvested under light, ground to a fine powder at the temperature of liquid nitrogen, and extracted in the medium of Scheibe and Stitt (1988) supplemented with 5 mM DTT. Activities were assayed immediately after extraction using the conditions of Kossmann et al. (1994) for FBPase and PRK and the conditions of Scheibe and Stitt (1988) for NADP-MDH. Total activities of the three enzymes were determined after reduction with 50 mM DTT for 1 h at 25°C.

In vitro Prx reduction was performed in a reconstituted system consisting of 0.5 mM NADPH, 0.5 μM pea FNR, 1 μM spinach (*Spinacia oleracea*) FTR, 5 to 10 μM Trx *f*, *m*, or *x* from spinach, 1 μM 2-Cys Prx B from *Arabidopsis thaliana*, and the indicated concentrations of either pea Fd or *Anabaena* Fld in 30 mM Tris-HCl, pH 8.0. After 15 min at 30°C, the reaction was quenched with 10 mM *N*-ethylmaleimide and the redox state of Prx was evaluated by nonreducing SDS-PAGE and immunoblotting (König et al., 2002). Rates of H_2O_2 reduction were measured in the same reconstituted medium described above, except that Prx and Fld were 4 and 10 μM, respectively. The assay was initiated by the addition of H_2O_2 to 50 μM, and the rates of H_2O_2 consumption were determined by reaction with xylenol orange as recommended by the manufacturer (Bioxytech H2O2-560; Bio-Stat).

Two-Dimensional Gel Electrophoresis

To detect the levels of inactivated Prx in vivo, leaf tissue was collected at the end of the treatment and/or illumination periods, freeze-clamped, and extracted essentially as described above for the chloroplast enzymes. Aliquots corresponding to 8 to 16 μg of total soluble protein, derivatized

or not with 10 mM *N*-ethylmaleimide, were resolved by nonreducing SDS-PAGE on 15% polyacrylamide gels followed by immunoblot detection (König et al., 2002).

For two-dimensional gel electrophoresis, lysates corresponding to 15 μg of protein were applied to precast vertical isoelectric focusing gels (pH 3 to 7; Novex, Invitrogen). Focusing, processing, and reduction of the isoelectric focusing strips and second-dimension SDS-PAGE on 15% polyacrylamide gels were performed as recommended by the manufacturer. Prx spots were visualized after transfer to nitrocellulose membranes and reaction with specific antisera.

Analytical Procedures

Intact chloroplasts were isolated from wild-type and transgenic plants using Percoll gradient centrifugation (Wu et al., 1991). Chlorophyll in leaves and chloroplasts was determined spectrophotometrically in acetone extracts (Lichtenthaler, 1987). Limited proteolysis of isolated chloroplasts (corresponding to 2 mg chlorophyll/mL) was performed by incubation for 30 min with 100 μg/mL thermolysin in ice-cold 50 mM HEPES-KOH and 330 mM sorbitol. The reaction was stopped by the addition of EDTA to 10 mM, and the plastids were reisolated by centrifugation through silicone oil layers (Serra et al., 1995). Digestion of broken chloroplasts was performed under the same conditions, but the plastids were previously shocked by incubation for 10 min at 20°C in 20 mM Tris-HCl, pH 8.0, 1 mM EDTA, and the reisolation step was omitted. Detection of Fld, Fd, Rubisco LSU, PFP, and the cytosolic isoform of NAD-MDH in whole leaf and chloroplast extracts was performed by SDS-PAGE and immunoblotting using 15% polyacrylamide gels and polyclonal antisera.

For the determination of ROS and antioxidant metabolites, attached leaves from node 9 of soil-cultured 2-month-old plants were sprayed with 30 μM MV and illuminated at 500 $\mu mol \cdot m^{-2} \cdot s^{-1}$. Leaves were incubated at 40°C under the same light intensity or irradiated with 1200 $\mu mol \cdot m^{-2} \cdot s^{-1}$. Incubations were prolonged for 18 h in all cases, and controls were kept in the growth chamber for the same period. At the end of the treatments, leaves from the susceptible lines displayed mild symptoms of wilting, whereas chlorosis was only marginal. The tissue was ground in liquid nitrogen, and the contents of superoxide and H_2O_2 were estimated in cleared lysates by measuring lucigenin- and luminol-dependent chemiluminiscence, respectively (Bolwell et al., 1998; Dat et al., 1998). MDA levels were determined by HPLC after reaction with thiobarbituric acid (Templar et al., 1999). Ascorbate and thiols were assayed in leaf extracts by colorimetric methods using the extraction procedures and conditions reported by Foyer et al. (1995).

Accession Number

Sequence data from this article can be found in the GenBank/EMBL data libraries under accession number S68006.

Supplemental Data

The following materials are available in the online version of this article.

Supplemental Figure 1. Purified *Anabaena* Fld Mediates $NADP^+$ Photoreduction by Tobacco Thylakoids.

Supplemental Figure 2. Accumulation of Fld in Transgenic Tobacco Plants.

Supplemental Figure 3. MV Toxicity in Leaf Discs from Wild-Type and Fld-Expressing Plants.

Supplemental Figure 4. Increased Tolerance of Transgenic Tobacco Plants Expressing Bacterial Fld in Chloroplasts to Different Sources of Environmental Stress.

Supplemental Figure 5. Effect of Fld Accumulation on the Patterns of Leaf Antioxidant Enzyme Isoforms.

Supplemental Figure 6. The Levels of Components of the Trx/FTR Pathway Are Not Affected by Fld Expression or Stress.

Supplemental Table 1. Phenotypic Analysis of Wild-Type and Transgenic Tobacco Plants Expressing Fld in Chloroplasts.

Supplemental Table 2. Effect of Fld Expression on the Levels of Antioxidant Enzymes and Metabolites in Plants Exposed to MV.

Supplemental Table 3. Fld Expression Prevents Overoxidation of 2-Cys Prx in Stressed Tobacco Plants.

Supplemental Table 4. Effect of Fld Expression on the Activation State of Trx-Dependent Chloroplast Enzymes in Plants Subjected to Stress Conditions.

ACKNOWLEDGMENTS

We are indebted to our colleagues from the National University of Rosario, Argentina: José Pellegrino (Instituto de Fisiología Experimental), María Mamprin (Pharmacology Unit), and Ramiro Rodriguez (Instituto de Biología Molecular y Celular de Rosario) for their assistance in ROS, thiol, and MDA determinations, respectively; Eligio Morandi (Agronomy School) for his invaluable help with the water-deficit and UV-C experiments; and Mercedes Leiva for statistical analyses. We also thank Karl-Josef Dietz (Bielefeld University, Germany) for the generous gift of 2-Cys Prx B from *Arabidopsis* and its specific polyclonal antiserum; Peter Schürmann (Neuchâtel University, Switzerland) for spinach Trx *f*, Trx *m*, and FTR; Myroslava Miginiac-Maslow (Université de Paris-Sud, France) for Trx *x*; and Florencio Podestá (Centro de Estudios Fotosintéticos y Bioquímicos, National University of Rosario, Argentina) for the antibodies against pineapple MDH and potato PFP. This research was supported by grants from Agencia Nacional de Promoción Científica y Tecnológica, the Consejo Nacional de Investigaciones Científicas y Técnicas, and the Fundación Antorchas, Argentina.

Received March 10, 2006; revised May 15, 2006; accepted June 8, 2006; published July 7, 2006.

REFERENCES

Allen, R.D. (1995). Dissection of oxidative stress tolerance using transgenic plants. Plant Physiol. **107,** 1049–1054.

Apel, K., and Hirt, H. (2004). Reactive oxygen species: Metabolism, oxidative stress and signal transduction. Annu. Rev. Plant Biol. **55,** 373–399.

Arabidopsis Genome Initiative (2000). Analysis of the genome sequence of the flowering plant *Arabidopsis thaliana*. Nature **408,** 796–815.

Backhausen, J.E., Kitzmann, C., Horton, P., and Scheibe, R. (2000). Electron acceptors in isolated intact spinach chloroplasts act hierarchically to prevent over-reduction and competition for electrons. Photosynth. Res. **42,** 75–86.

Baier, M., Noctor, G., Foyer, C.H., and Dietz, K.J. (2000). Antisense suppression of 2-Cys peroxiredoxin in *Arabidopsis thaliana* specifically enhances the activities and expression of enzymes associated with ascorbate metabolism but not glutathione metabolism. Plant Physiol. **124,** 823–832.

Baker, N.R., and Rosenqvist, E. (2004). Applications of chlorophyll fluorescence can improve crop production strategies: An examination of future possibilities. J. Exp. Bot. **403,** 1607–1621.

Balmer, Y., Koller, A., del Val, G., Manieri, W., Schürmann, P., and Buchanan, B.B. (2003). Proteomics gives insight into the regulatory function of chloroplast thioredoxins. Proc. Natl. Acad. Sci. USA **100,** 370–375.

Balmer, Y., Vensel, W.H., Tanaka, C.K., Hurkman, W.J., Gelhaye, E., Rouhier, N., Jacquot, J.-P., Manieri, W., Schürmann, P., Droux, M., and Buchanan, B.B. (2004). Thioredoxin links redox to the regulation of fundamental processes of plant mitochondria. Proc. Natl. Acad. Sci. USA **101,** 2642–2647.

Beauchamp, C., and Fridovich, I. (1971). Superoxide dismutase: Improved assays and an assay applicable to acrylamide gels. Anal. Biochem. **44,** 276–287.

Bohme, H. (1978). Quantitative determination of ferredoxin, ferredoxin-$NADP^+$ reductase and plastocyanin in spinach chloroplasts. Eur. J. Biochem. **83,** 137–141.

Bolwell, G.P., Davies, D.R., Gerrish, C., Auh, C.K., and Murphy, T.M. (1998). Comparative biochemistry of the oxidative burst produced by rose and French bean cells reveals two distinct mechanisms. Plant Physiol. **116,** 1379–1385.

Broin, M., and Rey, P. (2003). Potato plants lacking the CDSP32 plastidic thioredoxin exhibit overoxidation of the BAS1 2-cysteine peroxiredoxin and increased lipid peroxidation in thylakoids under photooxidative stress. Plant Physiol. **132,** 1335–1343.

Buchanan, B.B., Schürmann, P., Wolosiuk, R.A., and Jacquot, J.-P. (2002). The ferredoxin/thioredoxin system: From discovery to molecular structures and beyond. Photosynth. Res. **73,** 215–222.

Collin, V., Issakidis-Bourguet, E., Marchand, C., Hirasawa, M., Lancelin, J.M., Knaff, D.B., and Miginiac-Maslow, M. (2003). The *Arabidopsis* plastidial thioredoxins: New functions and new insights into specificity. J. Biol. Chem. **278,** 23747–23752.

Dat, J.F., López-Delgado, H., Foyer, C.H., and Scott, I.M. (1998). Parallel changes in H_2O_2 and catalase during thermotolerance induced by salicylic acid or heat acclimation in mustard seedlings. Plant Physiol. **116,** 1351–1357.

Erdner, D.L., Price, N.M., Doucette, G.J., Peleato, M.L., and Anderson, D.M. (1999). Characterization of ferredoxin and flavodoxin as markers of iron limitation in marine phytoplankton. Mar. Ecol. Prog. Ser. **184,** 43–53.

Falk, S., Samson, G., Bruce, D., Huner, N.P.A., and Laudenbach, D.E. (1995). Functional analysis of the iron-stress induced CP 43′ polypeptide of PS II in the cyanobacterium *Synechococcus* sp PCC 7942. Photosynth. Res. **45,** 51–60.

Fillat, M.F., Borrias, W.E., and Weisbeek, P.J. (1991). Isolation and overexpression in *Escherichia coli* of the flavodoxin gene from *Anabaena* PCC 7119. Biochem. J. **280,** 187–191.

Foyer, C.H., Souriau, N., Perret, S., Lelandais, M., Kunert, K.J., Pruvost, C., and Jouanin, L. (1995). Overexpression of glutathione reductase but not glutathione synthetase leads to increases in antioxidant capacity and resistance to photoinhibition in poplar trees. Plant Physiol. **109,** 1047–1057.

Gallois, P., and Marinho, P. (1995). Leaf disk transformation using *Agrobacterium tumefaciens*-expression of heterologous genes in tobacco. Methods Mol. Biol. **49,** 39–48.

Geiger, M., Haake, V., Ludewig, F., Sonnewald, U., and Stitt, M. (1999). The nitrate and ammonium nitrate supply have a major influence on the response of photosynthesis, carbon metabolism, nitrogen metabolism and growth to elevated carbon dioxide in tobacco. Plant Cell Environ. **22,** 1177–1199.

Gupta, A.S., Webb, R.P., Holaday, A.S., and Allen, R.D. (1993). Overexpression of superoxide dismutase protects plants from oxidative stress. Plant Physiol. **103,** 1067–1073.

Hagemann, M., Jeanjean, R., Fulda, S., Havaux, M., Joset, F., and Erdmann, N. (1999). Flavodoxin accumulation contributes to enhanced cyclic electron flow around photosystem I in salt-stressed cells of *Synechocystis* sp. strain PCC 6803. Physiol. Plant. **105,** 670–678.

Hajdukiewicz, P., Svab, Z., and Maliga, P. (1994). The small, versatile pPZP family of *Agrobacterium* binary vectors for plant transformation. Plant Mol. Biol. **25,** 989–994.

Hanke, G.T., Kimata-Ariga, Y., Taniguchi, I., and Hase, T. (2004). A post genomic characterization of Arabidopsis ferredoxins. Plant Physiol. **134,** 255–264.

Holt, N.E., Fleming, G.R., and Niyogi, K.K. (2004). Toward an understanding of the mechanism of nonphotochemical quenching in green plants. Biochemistry **43,** 8281–8289.

Holtgrefe, S., Bader, K.P., Horton, P., Scheibe, R., von Schaewen, A., and Backhausen, J.E. (2003). Decreased content of leaf ferredoxin changes electron distribution and limits photosynthesis in transgenic potato plants. Plant Physiol. **133,** 1768–1778.

Inda, L.D., and Peleato, M.L. (2002). Immunoquantification of flavodoxin and ferredoxin from *Scenedesmus vacuolatus* (Chlorophyta) as iron-stress molecular markers. Eur. J. Phycol. **37,** 579–586.

Knaff, D.B. (2005). Ferredoxin and ferredoxin-dependent enzymes. In Oxygenic Photosynthesis: The Light Reactions, D.R. Ort and C.F. Yocum, eds (Dordrecht, The Netherlands: Kluwer Academic Publishers), pp. 333–361.

König, J., Baier, M., Horling, F., Kahmann, U., Harris, G., Schürmann, P., and Dietz, K.J. (2002). The plant-specific function of 2-Cys peroxiredoxin-mediated detoxification of peroxides in the redox-hierarchy of photosynthetic electron flux. Proc. Natl. Acad. Sci. USA **99,** 5738–5743.

Kossmann, J., Sonnewald, U., and Willmitzer, L. (1994). Reduction of the chloroplastic fructose-1,6-bisphosphatase in transgenic potato plants impairs photosynthesis and plant growth. Plant J. **6,** 637–650.

Kramer, D.M., Avenson, T.J., and Edwards, G.E. (2004). Dynamic flexibility in the light reactions of photosynthesis governed by both electron and proton transfer reactions. Trends Plant Sci. **9,** 349–357.

Lichtenthaler, H.K. (1987). Chlorophylls and carotenoids: Pigments of photosynthetic biomembranes. Methods Enzymol. **148,** 350–382.

Mazouni, K., Domain, F., Chauvat, F., and Cassier-Chauvat, C. (2003). Expression and regulation of the crucial plant-like ferredoxin of cyanobacteria. Mol. Microbiol. **49,** 1019–1029.

Mittler, R., and Zilinskas, B.A. (1993). Detection of ascorbate peroxidase activity in native gels by inhibition of the ascorbate-dependent reduction of nitroblue tetrazolium. Anal. Biochem. **212,** 540–546.

Munekage, Y., Hashimoto, M., Miyake, C., Tomizawa, K., Endo, T., Tasaka, M., and Shikanai, T. (2004). Cyclic electron flow around PSI is essential for photosynthesis. Nature **429,** 579–582.

Nogués, I., Tejero, J., Hurley, J.K., Paladini, D., Frago, S., Tollin, G., Mayhew, S.G., Gómez-Moreno, C., Ceccarelli, E.A., Carrillo, N., and Medina, M. (2004). Role of the C-terminal tyrosine of ferredoxin-nicotinamide adenine dinucleotide phosphate reductase in the electron transfer processes with its protein partners ferredoxin and flavodoxin. Biochemistry **43,** 6127–6137.

Petracek, M.E., Dickey, L.F., Nguyen, T.T., Gatz, C., Sowinski, D.A., Allen, G.C., and Thompson, W.F. (1998). Ferredoxin-1 mRNA is destabilized by changes in photosynthetic electron transport. Proc. Natl. Acad. Sci. USA **95,** 9009–9013.

Pietrzak, M., Shillito, R.D., Hohn, T., and Potrykus, I. (1986). Expression in plants of two bacterial antibiotic resistance genes after protoplast transformation with a new plant expression vector. Nucleic Acids Res. **14,** 5857–5868.

Scheibe, R. (2004). Malate valves to balance cellular energy supply. Physiol. Plant. **120,** 21–26.

Scheibe, R., and Stitt, M. (1988). Comparison of NADP-malate dehydrogenase activation, QA reduction and O_2 evolution in spinach leaves. Plant Physiol. Biochem. **26,** 473–481.

Serra, E.C., Krapp, A.R., Ottado, J., Feldman, M.F., Ceccarelli, E.A., and Carrillo, N. (1995). The precursor of pea ferredoxin-$NADP^+$ reductase synthesized in *Escherichia coli* contains bound FAD and is transported into chloroplasts. J. Biol. Chem. **270,** 19930–19935.

Singh, A.K., Li, H., and Sherman, L.A. (2004). Microarray analysis and redox control of gene expression in the cyanobacterium *Synechocystis* sp. PCC 6803. Physiol. Plant. **120,** 27–35.

Teige, M., Melzer, M., and Süss, K.H. (1998). Purification, properties and *in situ* localization of the amphibolic enzymes D-ribulose 5-phosphate 3-epimerase and transketolase from spinach chloroplasts. Eur. J. Biochem. **252,** 237–244.

Templar, J., Kon, S.P., Milligan, T.P., Newman, D.J., and Raftery, M.J. (1999). Increased plasma malondialdehyde levels in glomerular disease as determined by a fully validated HPLC method. Nephrol. Dial. Transplant. **14,** 946–951.

Wood, Z.A., Poole, L.B., and Karplus, P.A. (2003). Peroxiredoxin evolution and the regulation of hydrogen peroxide signaling. Science **300,** 650–653.

Wu, J., Neimanis, S., and Heber, U. (1991). Photorespiration is more effective than the Mehler reaction in protecting the photosynthetic apparatus against photoinhibition. Bot. Acta **104,** 283–291.

Yousef, N., Pistorius, E.K., and Michel, K.P. (2003). Comparative analysis of *idiA* and *isiA* transcription under iron starvation and oxidative stress in *Synechococcus elongatus* PCC 7942 wild-type and selected mutants. Arch. Microbiol. **180,** 471–483.

Zheng, M., Doan, B., Schneider, T.D., and Storz, G. (1999). *OxyR* and *SoxRS* regulation of *fur*. J. Bacteriol. **181,** 4639–4643.

Zimmermann, P., Hirsch-Hoffmann, M., Hennig, L., and Gruissem, W. (2004). GENEVESTIGATOR. Arabidopsis microarray database and analysis toolbox. Plant Physiol. **136,** 2621–2632.